Jpn. J. Appl. Phys. Vol. 41 (2002) pp. 3974–3977
Part 1, No. 6A, June 2002

Simultaneous Atomic Force Microscope and Quartz Crystal Microbalance Measurements: Interactions and Displacement Field of a Quartz Crystal Microbalance

J.-M. FRIEDT, K. H. CHOI, L. FRANCIS and A. CAMPITELLI

IMEC, Kapeldreef 75, 3001 Leuven, Belgium

(Received January 22, 2002; accepted for publication February 25, 2002)

We analyze the interaction of two instruments often used in material science analysis, the atomic force microscope (AFM) and the quartz crystal microbalance (QCM), here combined in a single instrument for simultaneous measurements on a single sample. We show, using finite element analysis, that the in-plane displacement of a QCM oscillating in liquid with a quality factor of 2000 is 2 nm. The out-of-plane displacement is about one tenth of the in-plane displacement. This latter effect, due to the finite size of the electrodes, results in longitudinal acoustic waves launched in the liquid surrounding the QCM. If bounced against an obstacle, in our case the AFM cantilever holder, these longitudinal waves create standing wave patterns which cause frequency fluctuations of the resonator when it is moved, and thus decrease the QCM sensitivity.
[DOI: 10.1143/JJAP.41.3974]

KEYWORDS: QCM, displacement, resonance frequency, quality factor, AFM

1. Introduction

During the development of a combined quartz crystal microbalance[1] (QCM) — atomic force microscope[2] (AFM) instrument, we faced the challenge of estimating the displacement of the QCM resonator parallel to the electrode plane (which defines the lateral resolution of our AFM imaging) and normal to the electrode plane (which defines the topography resolution of the AFM scans).

Simultaneous AFM and QCM measurements of a sample allow the following:

- differents kinds of data to be gathered on different scales (cm^2 scale in the case of the QCM, nm^2 scale in the case of the AFM) and of a very different nature (mass change/viscosity losses in the case of the QCM, topography/stiffness in the case of the AFM). These measurements are performed on a single sample and thus it is guaranteed that the same conditions are met during the data gathering, which might not be evident for successive experiments with various instruments.
- checking of the validity and assumptions in converting frequency shifts and quality factor (damping) variations as measured by the QCM to mass changes (using the Sauerbrey equation).

Although the combination of several measurement techniques has shown promising progress by obtaining complementary results,[3] simultaneous measurements using AFM and QCM have not yet been performed to our knowledge.

We focused on precisely modeling the finite counter electrode size in order to accurately predict the out-of-plane displacement which also leads to frequency fluctuations when an obstacle (AFM cantilever holder) is brought close to the QCM surface because of the acoustic longitudinal waves generated in the liquid medium.[4]

2. Simulation Tools

We used the open-source software Modulef,[5] latest release as of September 2001, developed by INRIA (France) for simulating a cylindrical AT-cut quartz crystal resonator patterned with finite sized electrodes.

The piezoelectric properties of quartz were defined using the tabulated values found in ref. 6 and rotated to fit the AT cut using the formula provided by ref. 7.

3. Static Simulations

Our first approach is to apply a DC voltage between the electrodes deposited on opposite surfaces of the quartz resonator. We monitor the spatial distribution of the displacement field while keeping the position of the sensing electrode fixed.

We simulate a 14-mm-diameter quartz resonator 400 μm thick, fitted with a 5-mm-diameter massless counter electrode on which the DC potential (0.5 V, Fig. 2 left) is applied while the sensing electrode completely covers the top side of the QCM and is grounded. The total number of points used for this 3D simulation is 3320, which define 2040 pentaedral finite elements and 1280 hexaedral elements (Fig. 1). The results of this simulation are as follows:

- the maximum static displacement in the X direction is 1.075 pm, Fig. 3, left,
- the maximum static displacement in the Y direction is 0.126 pm, Fig. 3, right, and
- the maximum static displacement in the Z direction is 0.102 pm, Fig. 2, right.

As expected from an analytical resolution for an infinite plate, the displacement field is mainly oriented in the X axis direction (Fig. 1, right).

Inside the volume defined by a vertical cylinder above the counter electrode, the displacement is mainly parallel to the X direction, while discrepencies in this behaviour appear on the frontier of the counter electrode. These results for the X direction are in close agreement with previous analytical results presented in refs. 8–10 and they bring new insight to the Z displacement of the QCM which cannot be analyzed using an analytical formula which assumes an infinite electrode surface. The displacement normal to the electrode plan, about one tenth of the in-plane displacement, is much larger than previously estimated[9] and explains the origin of the large component of longitudinal waves generated by the QCM in the surrounding liquid.

4. Dynamic Simulations

With the intention of achieving conditions closer to the experimental conditions, a simulation of the dynamic oscillation of the quartz resonator should be performed in

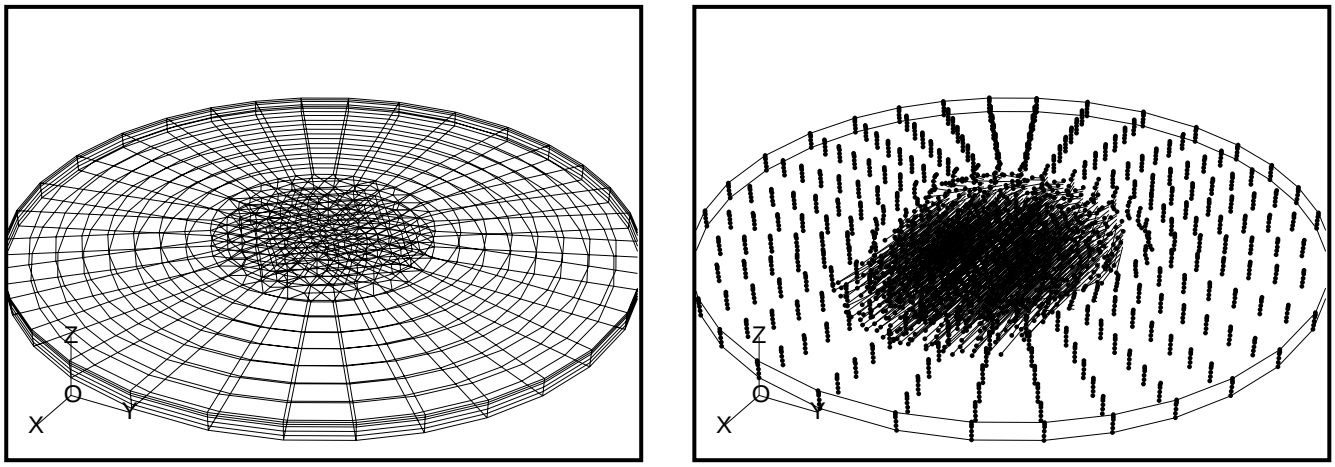

Fig. 1. Final 3D structure after defining the mesh (left), and the displacement field after resolution of the problem (right).

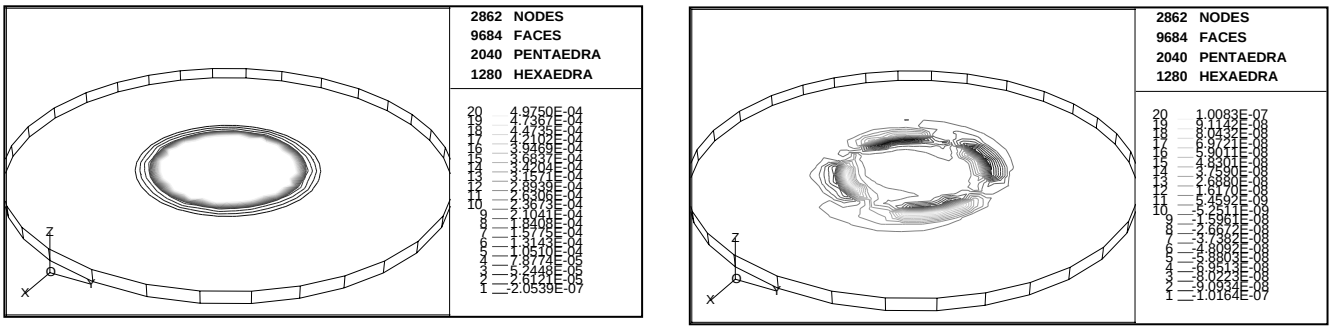

Fig. 2. Display of the DC potential (voltage, in kV) distribution (equipotential lines range from 0.5 V to -0.2 mV) and the amplitude of the out-of-plane (Z) displacement (equidisplacement lines range from 0.1 pm to -0.1 pm).

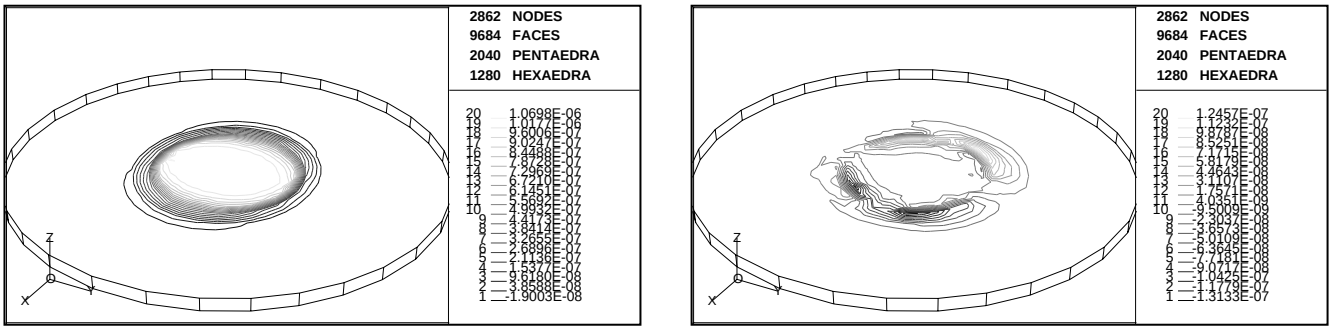

Fig. 3. Display of the amplitude of the displacement in the two in-plane directions (main displacement axes X and Y). Lines of equal displacement are displayed in μm.

order to directly obtain the displacement field enhanced by the mechanical resonance. This approach presents two major difficulties:

- in a simulation without damping, the displacement field for any frequency other than the resonance frequency is the same as in the DC mode, and the displacement field is expected to diverge when the resonance frequency is met.
- when including the damping, the losses that are dependent on the experimental conditions and the imaginary part η_{ij} ($i,j \in [1,6]$) of the stiffness constants (i.e., the damping coefficient) are extremely difficult to estimate. Using the relation[7] $\eta_{ij} = C_{ij}/(Q_{ij}\omega_0)$, where $Q_{ij} = Q$ is the quality coefficient (estimated to be equal to the experimentally observed quality factor Q for all i and j), ω_0 the mechanical resonance pulsation and C_{ij} the real part of the mechanical stiffness constants, leads to a conclusion similar to enhancing the static displacement field by a factor Q[9] for estimating the dynamic displacement field.

Hence, we have not focused on obtaining additional results using dynamic mode simulations which are not expected to display any new results compared to the static mode simulation, and we now extend the results obtained from simulations with a DC electrical field to the dynamic oscillation by introducing the quality factor Q.

Following these conclusions, we extend the static results to the dynamic behaviour expected to occur at resonance by using[9] the formula $A_{\text{dynamic}} = A_{\text{static}} \times Q$, where A_{dynamic} is the oscillation amplitude at resonance and A_{static} is the previously computed DC displacement. Since we observe that our QCMs display quality factors in the 1000 to 3000 range when oscillating in liquid at the resonance frequency (4.7 MHz), the results are as follows (for $Q = 2000$):

- the maximum dynamic displacement in the X direction is 2.1 nm,
- the maximum dynamic displacement in the Y direction is 0.25 nm, and
- the maximum dynamic displacement in the Z direction is 0.20 nm.

These results are in agreement, once normalized for the quality factor, with the measurements obtained by Borovsky *et al.* using an STM under vacuum.[11]

5. Experimental QCM Frequency Fluctuations Measurements

We have designed a combined QCM-AFM instrument (Fig. 4) based on the scanning probe microscope developed by molecular imaging (Phoenix, USA), with the QCM probing electronics provided by Q-Sense AB (Göteborg, Sweden) and laboratory built quartz crystal resonators designed to oscillate at around 4.7 MHz by coating a 14-mm-diameter AT-cut quartz wafer with 50 nm Ti and 50 nm Au. The output amplitude of the Q-Sense instrument was measured to be in the 200 mV_{pp} range.

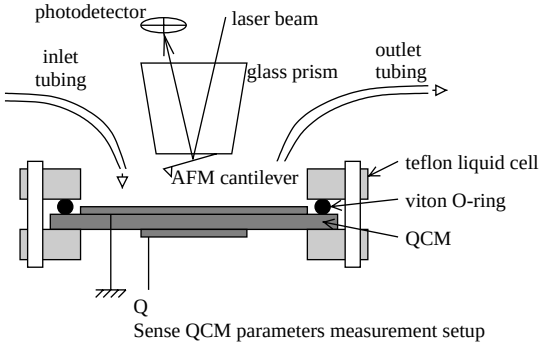

Fig. 4. Experimental setup of the combined QCM and AFM instrument, based on a commercial AFM designed by molecular imaging and a QCM parameter analysis instrument built by Q-Sense AB (Göteborg, Sweden).

We have experimentally (Fig. 5) observed in the combined QCM-AFM instrument the frequency drift of the QCM due to the AFM cantilever holder approach, as well as frequency fluctuations of the quartz crystal resonator during image scans ($1 \times 1\ \mu\text{m}^2$). We have observed that the first oscillation mode of the QCM (at 4.7 MHz) is the most sensitive to these environmental changes, as expected on the basis of its wider spread over the sensing electrode surface.[12]

Figures 5 and 6 display the influence of the position of the cantilever holder on the standing wave pattern generated between the QCM and cantilever holder surfaces, in the first case during the tip approach and in the second case during a protein adsorption experiment. The first mode appears to be much more sensitive to the disturbances due to environmental variations than the higher order modes (the third and fifth overtones were also measured during this study). As expected,[4] the peaks for the third mode are three times narrower and closer than the peak displayed for the first mode (since the wavelength of the standing wave is divided by 3 when the oscillation frequency is multiplied by 3).

6. Discussion

When used in combination with an AFM, the QCM will not visibly modify the image shape because of its oscillation. The step range of a typical 1-μm-wide, 256 pixel image is 4 nm, smaller than the in-plane oscillation of the quartz resonator. Similarly, the out-of-plane oscillation will not affect the resolution of the AFM for typical measurements in liquid. The main visible interactions are through the long-range longitudinal acoustic waves launched by the QCM which create standing wave patterns when reflected against the AFM cantilever holder. However, the tip displacement and position (tip-electrode distance) feedback then affect the frequency stability of the QCM and thus its sensitivity.

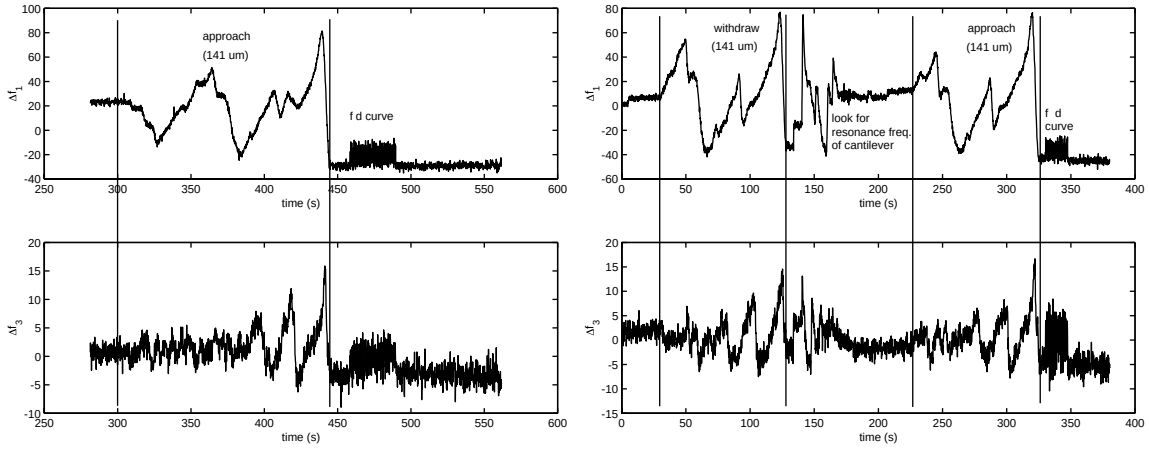

Fig. 5. Graphs displaying the effect of longitudinal waves on the frequency stability of the resonator (top graphs show the evolution of frequency of the first mode, bottom graphs show the evolution of frequency of the third mode). Total displacement during cantilever approach is 141 μm, which is quite close to the theoretical half-wavelength of an acoustic wave propagating in water at 5 MHz (152 μm.[4]).

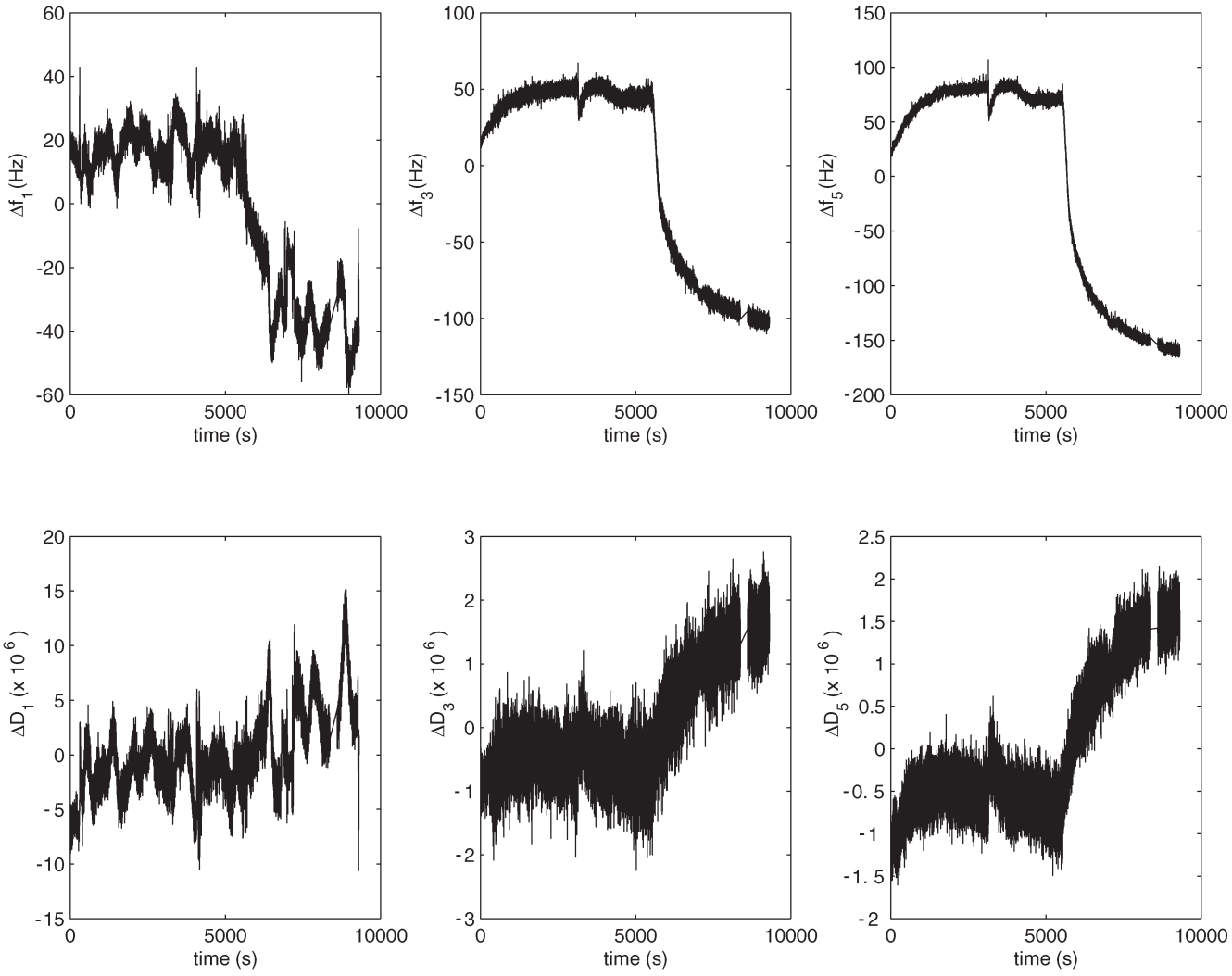

Fig. 6. Sensitivity of the various modes (1, 3 and 5 from left to right) of the QCM to environmental disturbances including hydrostatic pressure changes when inserting a new sample using the peristatic pump, image scans and protein adsorption (here 2.5 μg/ml human plasma fibrinogen at date 4075 and 15 to 20 μg/ml human plasma fibrinogen at date 5530) on the gold-coated grounded electrode. Top graphs show the frequency variations while bottom graphs display the changes in damping (inverse of the quality factor). The first mode is obviously the one most affected by environmental disturbances.

7. Conclusions

We have demonstrated the following using finite element analysis:

- the in-plane displacement of a resonator oscillating in liquid with a quality factor in the 1000 to 3000 range is at maximum in the nm range, typically 1 to 3 nm, when a 0.5 V_{pp} sine wave voltage is applied to the resonator, and
- the out-of-plane displacement of the resonator is about one tenth of that of the in-plane displacement. Such a conclusion leads, for a resonator oscillating in liquid with a quality factor in the 1000 to 3000 range, to an out-of-plane displacement in the angström range. This out of plane displacement is a direct reflection of the finite size of the counter electrode.

The out-of-plane oscillation results in longitudinal waves being emitted in the liquid, which create standing waves when they bounce off a planar obstacle parallel to the electrode located a few microns to a few hundred microns above the surface (depending on the position of the AFM cantilever holder during approach and scan). The interaction of the standing wave pattern and the crystal resonator is the source of the frequency fluctuations observed during the approach of the AFM cantilever holder towards the QCM surface.

1) A. Janshoff, H.-J. Galla and C. Steinem: Angew. Chem. Int. Ed. **39** (2000) 4004.
2) B. Drake, C. B. Prater, A. L. Weisenhorn, S. A. Gould, T. R. Albrecht, C. F. Quate, D. S. Cannell, H. G. Hansma and P. K. Hansma: Science **243** (1989) 1586.
3) P. Å. Ohlsson, T. Tjärnhage, E. Herbai, S. Löfås and G. Puu: Bioelectrochem. & Bioenerg. **38** (1995) 137.
4) Z. Lin and M. D. Ward: Anal. Chem. **67** (1995) 685.
5) http://www-rocq.inria.fr/modulef/
6) D. Royer and E. Dieulesaint: *Ondes élastiques dans les solides (tome 1)* (Masson, Paris, 1996) pp. 129 and 146 [in French].
7) B. A. Auld: *Acoustic Fields and Waves in Solids* (John Wiley & Sons, New York, 1973) Vol. 1, pp. 75, 170.
8) B. A. Martin and H. E. Hager: J. Appl. Phys. **65** (1989) 2627.
9) B. A. Martin and H. E. Hager: J. Appl. Phys. **65** (1989) 2630.
10) K. K. Kanazawa: Faraday Discuss. **107** (1997) 77.
11) B. Borovsky, B. L. Mason and J. Krim: J. Appl. Phys. **88** (2001) 4017.
12) A. C. Hillier and M. D. Ward: Anal. Chem. **64** (1992) 2539.